THE JOURNAL OF BIOLOGICAL CHEMISTRY VOL. 284, NO. 51, pp. 35758–35768, December 18, 2009

The Divalent Metal Transporter Homologues SMF-1/2 Mediate Dopamine Neuron Sensitivity in *Caenorhabditis elegans* Models of Manganism and Parkinson Disease*[S]

Received for publication, August 1, 2009, and in revised form, September 17, 2009 Published, JBC Papers in Press, September 30, 2009, DOI 10.1074/jbc.M109.051409

Raja Settivari[‡§], **Jennifer LeVora**[¶], **and Richard Nass**[‡§¶1]

From the [‡]*Department of Pharmacology and Toxicology,* [§]*Center for Environmental Health, and* [¶]*Stark Neuroscience Research Institute, Indiana University School of Medicine, Indianapolis, Indiana 46202*

Parkinson disease (PD) and manganism are characterized by motor deficits and a loss of dopamine (DA) neurons in the substantia nigra pars compacta. Epidemiological studies indicate significant correlations between manganese exposure and the propensity to develop PD. The vertebrate divalent metal transporter-1 (DMT-1) contributes to maintaining cellular Mn^{2+} homeostasis and has recently been implicated in Fe^{2+}-mediated neurodegeneration in PD. In this study we describe a novel model for manganism that incorporates the genetically tractable nematode *Caenorhabditis elegans*. We show that a brief exposure to Mn^{2+} increases reactive oxygen species and glutathione production, decreases oxygen consumption and head mitochondria membrane potential, and confers DA neuronal death. DA neurodegeneration is partially dependent on a putative homologue to DMT-1, SMF-1, as genetic knockdown or deletion partially inhibits the neuronal death. Mn^{2+} also amplifies the DA neurotoxicity of the PD-associated protein α-synuclein. Furthermore, both SMF-1 and SMF-2 are expressed in DA neurons and contribute to PD-associated neurotoxicant-induced DA neuron death. These studies describe a *C. elegans* model for manganism and show that DMT-1 homologues contribute to Mn^{2+}- and PD-associated DA neuron vulnerability.

Manganese is the second most prevalent transition metal and is an essential trace element that is necessary for normal growth and development. The heavy metal is required for a number of biological processes, including amino acid, lipid, and carbohydrate production, and metabolism, and is a cofactor for a diverse set of proteins, including arginases, transferases, hydrolases, ligases, and oxidoreductases (1, 2). Deficiencies in Mn^{2+}, although rare, have been linked with bone malformation, hypertension, osteoporosis, and epilepsy (3, 4).

Mn^{2+} is also a potent neurotoxicant, and occupational exposure to high concentrations of the metal can result in a neurological condition called manganism (1, 5). Symptoms of manganism include tremors, bradykinesia, rigidity, and facial muscle spasms (1, 6, 7). Mn^{2+} neurotoxicity has been associated with a number of occupational and environmental exposures. High incidence of manganism has been found in manganese miners and smelters (7–10). Welders appear to be particularly vulnerable to the disorder as manganese alloys used in the heating and joining of metals may result in the production and inhalation of manganese particles (11). Exposure to Mn^{2+}-based pesticides, including maneb and mancozeb, has also been associated with the development of manganism (12–14). Furthermore, significant environmental exposures have been reported with water contamination and possibly with the manganese-containing anti-knock fuel additive methylcyclopentadienyl manganese tricarbonyl (12). Recently, high exposures to Mn^{2+} have also been associated with psychoactive stimulant preparations for recreational drug use (15, 16).

Epidemiological studies suggest a significant correlation of exposure to high concentrations of Mn^{2+} and the propensity to develop Parkinson disease (PD)[2] (6, 11). PD is characterized by the loss of DA neurons in the substantia nigra and other basal ganglia (17). Individuals with occupational exposure to Mn^{2+} greater than 20 years have an increased probability to develop PD (18). Combinatorial long term exposures to Mn^{2+}, Fe^{2+}, and aluminum (greater than 30 years) have also been shown to lead to increased likelihood of PD (19). Acute Mn^{2+} toxicity results in symptoms similar (but not identical) to those seen in patients with PD, including rigidity, tremors, and bradykinesia (1, 7, 11, 20). As in PD, oxidative stress appears to play a significant role in the disorder, and the brain region most susceptible to Mn^{2+} injury is also sensitive to oxidative stress (21–26). Mn^{2+} toxicity can confer damage to the striatum, reduction of the DA precursor tyrosine hydroxylase, and DA neurodegeneration (27–29). The PD-associated pre-synaptic protein α-synuclein has also been proposed to contribute to the pathogenesis of both disorders (30–33). Although the molecular bases of manganism and Mn^{2+}-induced toxicity has not been elucidated, *in vitro* studies of Mn^{2+} treatments suggest inhibition of the

* This work was supported, in whole or in part, by National Institutes of Health Grants R011ES014459 and R01ES010563 from NIEHS. This work was also supported by Grant W81XWH-05-1-0239 from the Dept. of Defense Manganese Health Research Program (to R. N.).

[S] The on-line version of this article (available at http://www.jbc.org) contains supplemental Figs. S1–S3.

[1] To whom correspondence should be addressed: Dept. of Pharmacology and Toxicology, 635 Barnhill Drive, Indiana University School of Medicine, Indianapolis, IN 46202. Tel.: 317-278-8505; Fax: 317-274-7868; E-mail: ricnass@iupui.edu.

[2] The abbreviations used are: PD, Parkinson disease; DA, dopamine; DMT-1, divalent metal transporter-1; ROS, reactive oxygen species; GFP, green fluorescent protein; 6-OHDA, 6-hydroxy dopamine; RNAi, RNA interference; CEP, cephalic dendrite; H2-DCF-DA, 2,7-dichlorodihydrofluorescein diacetate; TMRE, tetramethyl rhodamine ethyl ester; WT, wild type; GAPDH, glyceraldehyde-3-phosphate dehydrogenase; NGM, nematode growth medium; DAT, dopamine transporter.

electron transport chain complex-I within the mitochondria and increase in production of reactive oxygen species (ROS) (21, 23, 34). Furthermore, there are significant changes in intracellular antioxidant levels, including GSH, thiols, and catalase (35, 36).

Mn^{2+} is believed to be transported into the cell via several routes, including voltage-gated and glutamate receptor calcium channels, the transferrin receptor, and the proton-coupled electrogenic divalent metal transporter-1, DMT-1 (37, 38). DMT-1 mediates the transport of divalent ions, including Mn^{2+}, Fe^{2+}, copper, cobalt, lead, and zinc. In yeast, DMT-1 isoforms Smf1p and Smf2p transport Mn^{2+} across the plasma membrane and intracellular vesicles, respectively (39–42). In vertebrates, two of four isoforms of DMT-1 have been identified and are the major transporters involved in absorption of Fe^{2+} in the intestines (37, 43). Also known as Nramp2 (natural resistance-associated macrophage protein), the transporters are expressed in most tissues and are capable of transporting divalent metal cations (38). Recently, DMT-1 has been implicated in Fe^{2+}-mediated DA neuronal death in PD and vertebrate model systems (44).

The nematode *Caenorhabditis elegans* is a powerful model system to explore the molecular basis of PD-associated DA neuronal vulnerability and death (45, 46). All of the genes responsible for DA biosynthesis, packaging, and reuptake have recognizable homologs in the worm genome, and genetic, cellular, and functional studies confirm their participation in dopaminergic function (47). Transcriptional green fluorescent protein (GFP) fusions allow the eight DA neurons to be clearly visible *in vivo* under a fluorescent dissecting scope, and, as in vertebrates, the neurotoxicants 6-hydroxy dopamine (6-OHDA), 1-methyl-4-phenylpyridinium, and rotenone can confer DA neurodegeneration (48, 49). Expression of human α-synuclein in *C. elegans* also confers DA neurodegeneration, aggregate formation, movement deficits, disruption of vesicle docking, and significant changes in gene expression of molecular pathways associated with the mitochondria and proteasome (50–52). Overexpression or mutations in other PD-associated genes also affect whole animal or DA neuron vulnerability (46, 53, 54).

In this study we describe a novel *in vivo* model for manganism. We show that a brief sub-lethal exposure of Mn^{2+} to *C. elegans* results in increases in ROS production and glutathione concentrations, a decrease in mitochondria membrane potential and oxygen consumption, and DA neurodegeneration. Mn^{2+} exposure also amplifies α-synuclein-induced DA neuronal death. DA neuron vulnerability to Mn^{2+} is partially dependent on the expression of DMT-1 homologue SMF-1 in DA neurons, because knockdown or deletion of the putative transporter partially protects against neuronal death. SMF-2, another DMT-1 homologue, is also expressed in DA neurons and contributes to the sensitivity to 6-OHDA, because knockdown or deletion of the protein partially protects against the DA cell death. These results suggest that the DMT-1 contributes to Mn^{2+}-induced DA neuron vulnerability in manganism and PD.

EXPERIMENTAL PROCEDURES

C. elegans Strains and Maintenance—The following strains were obtained from the *Caenorhabditis elegans* Genetics Center: wild-type Bristol N2, IG6 *smf-1(eh5) X*, VC171 *smf-2(gk133) X*, and RB1074 *smf-3(ok1035) IV*. The P_{dat1}::GFP strain is an integrated, transgenic line expressing GFP from behind the *dat-1* promoter and has been previously described (49, 50). This strain, now called BY250, was crossed into the mutant *smf-1–3* backgrounds and followed by PCR using genomic DNA and the following primers: *smf-1*-F, GAATTTTGCTTTGGCGTGTT; *smf-1*-R, TCAGTTTGGCACCACGTTAG; *smf-2*-F, CGGCTCCAAAAATGGAAATA; *smf-2*-R, GGGAAATCAGGTAAAAATGTGC *smf-3*F, TTCAGCTTGTCAAGGGCTTT; and *smf-3*-R, CTTCCATTGGGGAAGTTTGA. The resulting strains were generated: RJ907 (P_{dat-1}::GFP; *smf-1(eh5)*), RJ905 (P_{dat-1}::GFP; *smf-2(gk133)*), and RJ906 (P_{dat-1}::GFP; *smf-3(ok1035)*). Animals expressing human WT α-synuclein behind the *dat-1* promoter have previously been described (now called BY273 (P_{dat-1}::GFP; P_{dat-1}::$WT_{\alpha\text{-}synuclein}$). RJ928 is a genetic cross between BY250 and the RNA-mediated interference (RNAi)-sensitive NL2099 *rrf-3(pk1426*) nematodes. *C. elegans* strains were cultured on bacterial lawns of either OP-50 or NA-22 on NGM or 8P plates, respectively, at 20 °C according to standard methods (55, 56).

RNA Extraction and cDNA Synthesis—Total RNA was isolated from a synchronized *C. elegans* population using TRIzol reagent largely as described previously with minor modifications (57). Briefly, worm pellets after treatment with either $MnCl_2$ or 6-OHDA were resuspended in TRIzol (1 ml/100 μl of compact worm pellet). Protein and lipid impurities were separated from nucleic acids using chloroform, and RNA was precipitated with isopropyl alcohol. The RNA pellet was washed with 75% ethanol, air-dried, dissolved in RNase-free water, and stored at −80 °C until used. RNA concentrations were measured using an ND-1000 spectrophotometer (Nanodrop Technology, Wilmington, DE). One microgram of total RNA was reverse-transcribed to cDNA using oligo(dT) (IDT DNA, Coralville, IA), and reverse transcriptase (Bio Rad), following the manufacturer's instructions (cDNA synthesis kit, Bio-Rad). The cDNA was purified using Microcon YM30 filters (Millipore Corp., Bedford, MA) and measured using an ND-1000 spectrophotometer.

qPCR Measurements—Gene specific primers were designed using Primer3 software, and the primers were designed to be exon spanning to avoid amplification of contaminating genomic DNA. Glyceraldehyde-3-phosphate dehydrogenase (GAPDH) was selected as the housekeeping gene because its expression does not change as a result of $MnCl_2$ or 6-OHDA treatment. The following primers were used to determine changes in gene expression of smf-1, *smf-2*, or *smf-3* following Mn^{2+} exposure: smf-1 F, GTGGGTTTTGCTCTCAGCTC; smf-1 R, TGGCAATTGCTGTTCCAATA; smf-2 F, GCACTGGTTGGCTGATTTTT; smf-2 R, GGAGCATCCAGTTCCAGTGT; smf-3 F, GGAGTGCGAAAGTTTGAAGC; smf-3 R, TTGACAAGTGCCGAGTGAAG; GAPDH F, GAAACTGCTTCAACGCATCA; and GAPDH R, CCTTGGCGACAAGAAGGTAG. Real-time reaction was performed using 2× SYBR Green PCR master mix, using the ABI Prism 7500 sequence detection system (Applied Biosystems, Warrington, UK). Gene expression studies were performed in triplicate, and the formation of a single PCR product was confirmed using dissociation curves. Negative controls with the primers consisted of all of

the components of PCR mix except cDNA. Relative -fold change in gene expression for each gene was calculated using normalized C_T values (the cycle number at which the fluorescence passes the threshold).

Toxicant Exposures—Synchronized L1 stage worms were obtained by hypochlorite treatment of gravid adults followed by incubation of the embryos in M9 buffer for 18 h and washed at least 3× in dH_2O using standard protocols (49, 58). L1 stage worms (10 worms/μl) were incubated with dH_2O ± 50 mM manganese chloride ($MnCl_2$, Fisher Scientific, Fair Lawn, NJ), or 1% DMSO ± 5 mM 6-OHDA (Sigma-Aldrich, as previously described (58)) for 30 min at room temperature (~22 °C) with gentle mixing every 10 min. The light-sensitive 6-OHDA exposures were also performed in the dark. Following treatments, the worms were placed onto NGM/OP-50 plates and allowed to recover for 72 h at 20 °C. After recovery, 50–60 worms were immobilized on 2% agarose pads with 2% sodium azide and were scored for DA neurodegeneration under a fluorescence microscope (Leica MZ 16FA, Switzerland). Worms were scored positive for DA neuron degeneration when GFP in any part of the four cephalic dendrites (CEPs, which run from the nerve ring to tip of the nose) was absent (49). Each of the experiments was performed at least in triplicate, and the results are reported as means ± S.E. Osmotic control for $MnCl_2$ studies was treated with 75 mM potassium gluconate (Sigma-Aldrich), whereas controls were treated with 1% DMSO for 6-OHDA experiments.

GSH Analysis—Total glutathione levels were determined using the ApoGSH glutathione detection kit (BioVision, Palo Alto, CA) following the manufacturer's instructions with slight modifications. Briefly, synchronized L1 stage worms were exposed to 50 mM $MnCl_2$ and allowed to recover on NGM plates for 4 h at 20 °C. The worms were removed from the plates, and bacteria was removed from worms by three repeated washes and subsequent centrifugation. The worm pellet was homogenized by sonication, and the lysate was centrifuged at 14,000 rpm for 10 min at 4 °C. The supernatant was used for measuring total protein content and GSH levels. Monochlorobimane dye in the reaction forms adducts with GSH exclusively and fluoresces, whereas the unbound dye does not fluoresce. The intensity of the dye was measured at excitation and emission wavelengths of 380 and 460 nm, respectively. For each treatment group, at least three independent samples were prepared.

ROS Analysis—Total ROS formation was evaluated in the whole worm using 2,7-dichlorodihydrofluorescein diacetate (H2-DCF-DA). ROS oxidize the dye to the fluorescent 2,7-dichlorofluorescein, and the level of fluorescence corresponds to ROS cellular levels. ROS levels were determined following previously established protocols with slight modifications (59, 60). Briefly, synchronized L1 worms were exposed to $MnCl_2$ as described above, and washed 3× with water. The animals were resuspended in M9 at a concentration of 50,000 worms/ml, and 50 μl of the suspension was incubated in 50 μl of freshly prepared 100 μM H2-DCF-DA in four replicates in a 96-well plate. Control wells included worms from each treatment without H2-DCF-DA or wells containing H2-DCF-DA without worms. The basal fluorescent signal from each well was measured at excitation and emission wavelengths of 485 and 520 nm, respectively, using a spectrophotometer (Tecan Spectrafluor Plus). Following the addition of the worms, plates were incubated on a shaker at room temperature for 1 h and were measured under earlier conditions. Fluorescence values from the control wells were subtracted from the corresponding signal value of each well after the final measurement. All assays were performed in triplicates.

Mitochondrial Membrane Potential Analysis—Mitochondrial membrane potential was measured using the lipophilic cationic dye tetramethyl rhodamine ethyl ester (TMRE, Sigma) as previously described (61, 62). Following exposure to 50 mM $MnCl_2$, L1 stage worms were allowed to recover on NGM plates containing 0.1 μM TMRE for 48 h. The fluorescent images of the head region of each animal (from tip of nose to posterior end of terminal bulb) was captured using a Leica MZ 16FA fluorescence microscope, and the amount of dye accumulated was quantified using Image Pro Plus v6.2 software (Media Cybernetics, MD). The membrane potential of at least 20 live animals was evaluated in triplicate for each experimental condition.

Oxygen Consumption Analysis—Oxygen consumption was measured using a Mitocell MT200 respirometer and an oxygen electrode (Strathkelvin Instruments Ltd.) as previously described (60, 63). L1s were exposed to Mn^{2+} and allowed to recover on NGM plates at 20 °C for 48 h. Animals were then washed 3× with water and resuspended at a concentration of 6000 worms/ml. 60-μl aliquots were then transferred into the oxygen meter chamber, and the respiration rate was measured at 20 °C for 10 min. At least three independent experiments were performed comprising of at least three replicates per treatment group.

Antibodies and Immunohistochemistry—Antibodies to amino acids 1–61 and 428–465 from the putative *C. elegans* proteins SMF-1 (WP:CE37261) and SMF-2 (WP:CE02825), respectively, were generated using Genomic Antibody Technology at Strategic Diagnostics Inc. (Newark, DE). Rabbit polyclonal antibodies were further purified at Strategic Diagnostics Inc. Primary *C. elegans* cultures were prepared as previously described, but with slight modifications (64). Briefly, gravid adult worms were lysed with the synchronization solution as described earlier, and the egg pellet was washed using egg buffer (118 mM NaCl, 48 mM KCl, 2 mM $CaCl_2$, 2 mM $MgCl_2$, 25 mM HEPES), and the eggs were separated from the debris using a 60% sucrose solution. Eggs were digested using 4 mg/ml chitinase (Sigma), and embryonic cells were dissociated using syringe aspiration. Embryonic cells were then resuspended in L-15 medium (containing 10% fetal bovine serum and 1% penicillin/streptomycin) and grown on polylysine-coated slides at 20 °C. Following growth for 72 h, cells were fixed in 4% paraformaldehyde, permeabilized in 0.5% Triton X-100, and blocked using 1% normal goat serum. The cells were then incubated with either SMF-1 or SMF-2 primary antibodies (1:5000) at 4 °C overnight (14 h), followed by incubation with Texas Red-conjugated goat anti-rabbit secondary antibodies (Invitrogen, 1:5000) at room temperature for 1 h. Images were captured using confocal microscopy (Zeiss LSM 510 microscope).

RNA Interference—RNAi-sensitive NL2099 *rrf-3(pk1426)* nematodes were crossed into BY250 (65), and the resulting mutant strain (RJ928) was confirmed with PCR. RNAi experiments were carried out on NGM plates containing 1 mM isopropyl 1-thio-β-D-galactopyranoside and 100 μg/ml ampicillin and seeded with HT115 (DE3), an RNase III-deficient *Escherichia coli* strain carrying L4440 vector with the gene fragment (*smf-1* or *smf-2*) (GeneService, Source BioScience, PLC, Nottingham, UK) or empty vector (Addgene, Cambridge, MA) (66). Synchronized L1 stage RJ928 worms were transferred onto RNAi plates, and the feeding protocol was followed with slight modifications (67). 50–100 second generation gravid adults grown on RNAi bacteria were transferred to fresh RNAi media plates and allowed to lay eggs for 5 h. Adults were then removed from the plate. L1s hatched from the eggs (third generation) were exposed to Mn^{2+} or 6-OHDA as described above. The animals were allowed to recover on the RNAi plates for 72 h and evaluated as previously described (49).

RESULTS

Mn^{2+} Exposure Increases Oxidative Stress in C. elegans—To determine whether a brief exposure to Mn^{2+} may cause an increase in oxidative stress in *C. elegans*, we exposed young animals to 50 mM $MnCl_2$ for 30 min and determined whole animal GSH and ROS levels and oxygen consumption. Mitochondrial membrane potential changes were also evaluated in the head. One of the more important defenses against oxidative stress is the production of GSH, which reduces peroxides through GSH peroxidase-catalyzed reactions (68). GSH production has been observed to initially increase following exposures to a number of oxidants, including manganese and the dopamine-related metabolite quinone (21, 69). A brief exposure of *C. elegans* to 50 mM Mn^{2+} results in approximately a 5-fold increase in GSH levels 4 h post-exposure (Fig. 1*A*). These results indicate that *C. elegans* is sensitive to a single high level exposure to Mn^{2+} and are consistent with GSH activation in response to higher free radical levels. To determine whether an acute exposure to Mn^{2+} may cause a greater accumulation of ROS relative to non-exposed animals, we determined whole animal ROS levels using the ROS-dependent fluorescent dye DCF. L1 animals were resuspended in water with and without the addition of Mn^{2+}, and ROS levels were quantified 1 h later. We found that a brief exposure to Mn^{2+} caused a 2-fold increase in cellular ROS relative to non-Mn^{2+} exposed animals (Fig. 1*B*). These results are consistent with vertebrate studies that show that Mn^{2+} can increase cellular free radical production. A primary intracellular target of Mn^{2+} in vertebrates is mitochondria (1). Increases in ROS production can be due to Mn^{2+}-induced inhibition of complex I and activation of the permeability transition pore, resulting in the inefficient reduction of the final electron receptor and loss of mitochondrial membrane potential. To determine whether Mn^{2+} exposure may disrupt the mitochondrial membrane potential in the head region of *C. elegans*, we exposed control and Mn^{2+}-treated animals for 48 h to TMRE. TMRE is a mitochondrial-specific fluorescent dye whose rate of uptake is dependent on the mitochondria membrane potential (61). A single exposure to 50 mM Mn^{2+} resulted in a significant decrease in mitochondria membrane potential within the head relative to non-exposed nematodes (Fig. 1*C*). These results suggest that, as in vertebrate systems, Mn^{2+} may impair mitochondria function. To further explore whether Mn^{2+} may be toxic to mitochondria in *C. elegans*, we determined total cellular oxygen utilization following toxicant exposure. Reduction in cellular oxygen consumption has been correlated with dysfunctional mitochondria in vertebrates and *C. elegans* (63, 68). L1 animals were exposed to water either with or without Mn^{2+}, allowed to recover on plates containing bacteria for 48 h, and the respiration rate was determined. The rate of oxygen consumption for the Mn^{2+}-exposed worms was reduced greater than 2-fold relative to control, suggesting impaired mitochondrial function (Fig. 1*D*). The above results suggest that exposure of *C. elegans* to Mn^{2+} can confer significant oxidative stress and, as in vertebrate systems, is likely due to the accumulation of ROS and mitochondrial dysfunction.

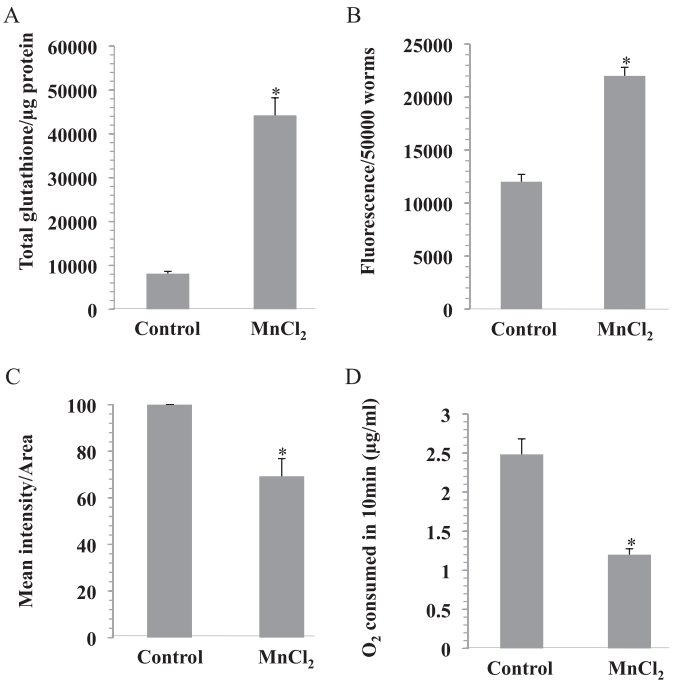

FIGURE 1. **Mn^{2+} exposure increases oxidative stress in *C. elegans*.** Synchronized L1 nematodes were treated with ± 50 mM $MnCl_2$ for 30 min then allowed to recover on NGM plates for 4 h, and total glutathione levels were evaluated (*A*). ROS levels were measured with or without Mn^{2+} treatment and incubation with DCF-DA for 60 min (*B*). Head mitochondrial membrane potential was determined following ± Mn^{2+} exposure and incubation with TMRE for 48 h. Head region images (from the nose to the posterior part of the terminal bulb) were captured using a Leica MZ 16FA fluorescence microscope, and fluorescent intensity of the dye was determined using Image Pro Plus v6.2 software (*C*). Oxygen consumption rate was measured following ± Mn^{2+} treatment using a Mitocell MT200 and Strathkelvin oxygen electrode (*D*). Shown are mean values ± S.E. of three individual replicates. *p* values were calculated using *t* test analysis. *, $p \leq 0.03$.

Exposure to Sub-lethal Concentrations of Mn^{2+} Confers DA Neurodegeneration—The DA neurons in vertebrates are particularly sensitive to oxidative stress and heavy metals, including Mn^{2+}, and DA neurodegeneration contributes to the behavioral phenotypes associated with manganism and PD. We previously generated transgenic worms that express GFP in the eight dopamine neurons in the hermaphrodite (49). These neurons are clearly visible under a fluorescent dissecting scope. We

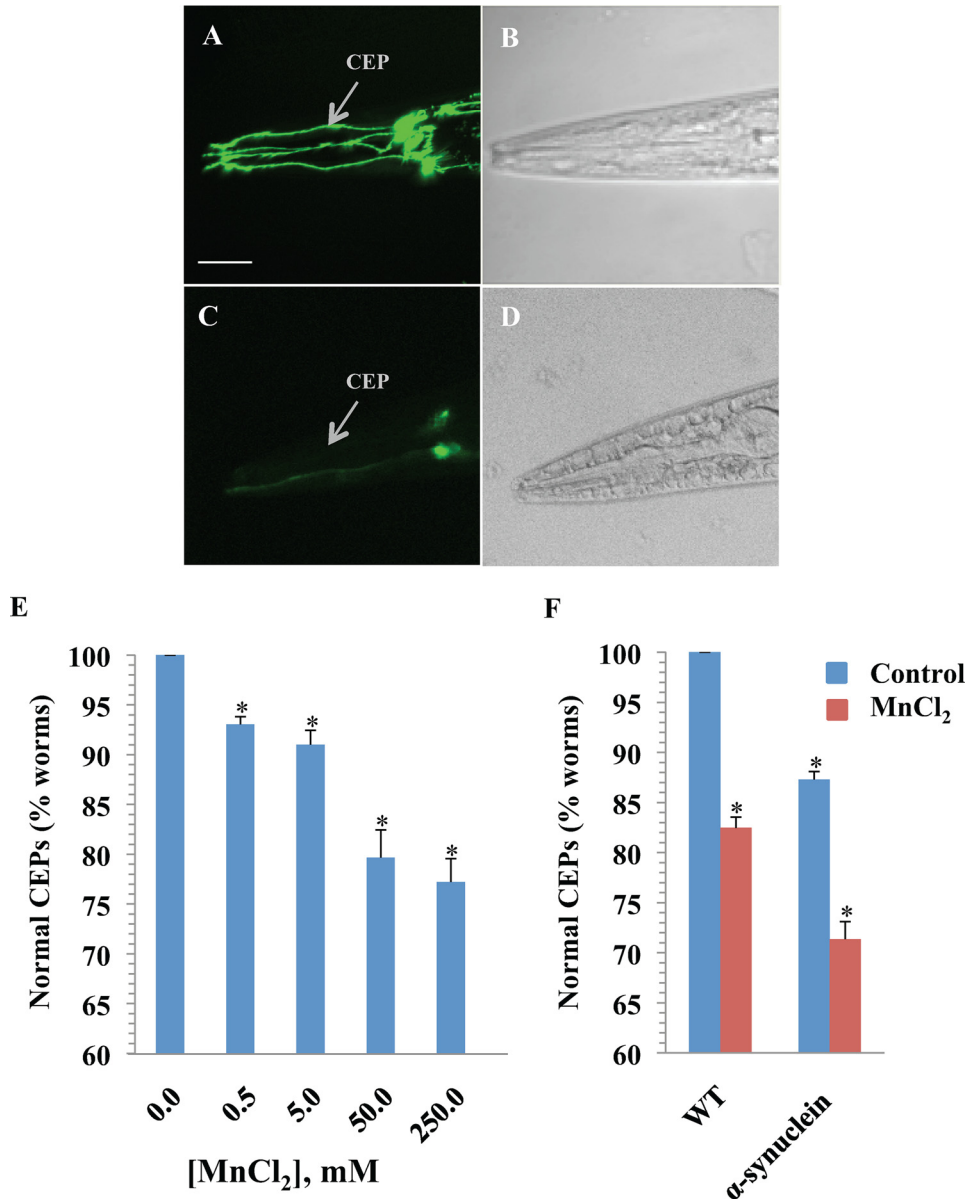

FIGURE 2. **Mn^{2+} confers DA neuron degeneration in WT and human α-synuclein-expressing nematodes.** *A*, GFP-expressing DA neurons (CEPs) within the head of a control worm exposed to water. Morphological changes were also not evident when exposed to the iso-osmotic solution of 75 mM potassium D-gluconate for the 50 mM exposures (data not shown). *B*, differential interference contrast image of the corresponding control animal. *C*, nematodes exposed to 50 mM $MnCl_2$ for 30 min and evaluated 72 h later; image chosen emphasizes significant loss of CEP cell bodies and dendrites. *D*, differential interference contrast image of the corresponding worms in *C*. *E*, quantitation of DA neuron integrity in WT animals or human α-synuclein expressing animals (*F*) following exposure to water or Mn^{2+}. Animals (≥50 worms/condition) were exposed to various concentrations of $MnCl_2$, and the GFP expression pattern in the CEP was examined 72 h later (see "Experimental Methods"). Anterior of the animal is to the *left*. *Scale bar* = 35 μm. Shown are mean values ± S.E. of at least three individual replicates. *p* values were calculated using *t* test analysis. *Asterisk* indicates $p = 0.03$ for all comparisons compared with controls (0.0 mM Mn^{2+}).

also demonstrated that a brief exposure of the animals to 6-OHDA results in a significant loss of DA neurons within the head (49). To determine whether exposure to Mn^{2+} may also cause DA neurodegeneration, we exposed *C. elegans* in liquid suspension to various concentrations of toxicant ranging from 0 to 250 mM for 30 min and transferred the animals to agar plates. We found that a brief exposure to the Mn^{2+} caused a significant loss of DA neurons within 72 h at all concentrations tested, and ~20% of the animals display DA neuron degeneration after exposure to 50 mM $MnCl_2$ (Fig. 2, *C* and *E*). This brief exposure does not result in any apparent long term changes in whole animal morphology or behavior, which suggests there is not large scale cellular dysfunction or death. The Mn^{2+}-induced DA neurodegeneration that we observed is similar to our prior studies in which we characterized the 6-OHDA-induced DA neurodegeneration by loss of dendritic GFP and loss of neuronal integrity by electron microscopy (49). In these studies, only the CEP processes that cannot be visually followed from the cell body to the tip of the nose are considered to have degeneration (49). Of those animals that demonstrate the neurodegeneration, on average we find one neuron (and sometimes more) that shows significant dendritic loss. We also observed other signs of DA neuron pathology such as the formation of neuronal blebs or a decrease in GFP intensity, even in animals that do not have an apparent loss of a dendrite, suggesting that there could be greater DA neuronal pathology than determined by loss of cellular integrity. To further evaluate the DA neuronal damage, we utilized high performance liquid chromatography analysis coupled to an electrochemical detection system to evaluate DA levels in Mn^{2+}-exposed worms relative to non-Mn^{2+}-exposed animals. A brief 30-min exposure to 50 mM Mn^{2+} followed by incubation on media growth plates at 20 °C for 48 h resulted in a loss of DA of ~60% in Mn^{2+}-exposed worms relatively to control animals (control worms = 33.15 ± 6.6 fmol/mg of wet weight, $n = 6$; Mn^{2+}-exposed worms = 13.20 ± 0.8 fmol/mg of wet weight, $n = 3$). The decrease in DA concentration is consistent with DA neuronal loss, because the DA neurons are the only cells that generate DA in *C. elegans* (47). Taken together, these results indicate that an acute Mn^{2+} exposure can cause degeneration of the *C. elegans* DA neurons.

Mn^{2+} Exposure Amplifies α-Synuclein-induced DA Neuronal Death—Mn^{2+} causes an increase in α-synuclein aggregation and fibrillation *in vitro* and *in vivo*, suggesting that Mn^{2+} may interact synergistically with α-synuclein to cause DA neuron dysfunction and pathology (30, 70). We have previously generated transgenic *C. elegans* strains expressing human

α-synuclein in DA neurons and find that WT and A53T α-synuclein expression confers DA neurodegeneration and the formation of inclusion-type bodies (50). To determine whether Mn^{2+} may amplify the toxicity of α-synuclein-induced DA neuronal death *in vivo*, we briefly exposed nematodes expressing human WT α-synuclein to 50 mM Mn^{2+}, and found a small, yet significant increase in DA neuronal death (Fig. 2*F*). These results are consistent with vertebrate studies that suggest that Mn^{2+} can amplify the toxicity conferred by α-synuclein and may exacerbate the α-synuclein-associated DA neuron dysfunction in PD and manganism.

Expression of the Putative DMT-1 Transcripts smf-1, smf-2 and smf-3 Are Modulated by Mn^{2+} Exposure—A primary mechanism for entry of Mn^{2+} into vertebrate cells is through divalent metal transporter, DMT-1 (38). A BLAST search with a human homologue of DMT-1 and a sequence alignment of the results using ClustalW2 suggest that *C. elegans* has three putative homologues to DMT-1: SMF-1–3 (percent similarity from 72 to 76%, with percent amino acid identity between 55 and 58%) (Fig. 3) (71, 72). The putative transporters are predicted to have 12 transmembrane domains and, consistent with vertebrates, a conserved consensus transport sequence located between transmembrane domains eight and nine (73). We hypothesized that, because Mn^{2+} confers oxidative stress and DA neuronal death, the Mn^{2+} transporters responsible for cellular uptake and storage may be tightly regulated. If cellular Mn^{2+} is tightly regulated in *C. elegans*, we further hypothesized that an acute sub-lethal exposure to Mn^{2+} may cause a significant change in gene expression of the putative transporters. We utilized quantitative PCR to determine gene expression levels in control and Mn^{2+}-exposed worms. Young nematodes exposed to 50 mM $MnCl_2$ for 30 min showed a significant and

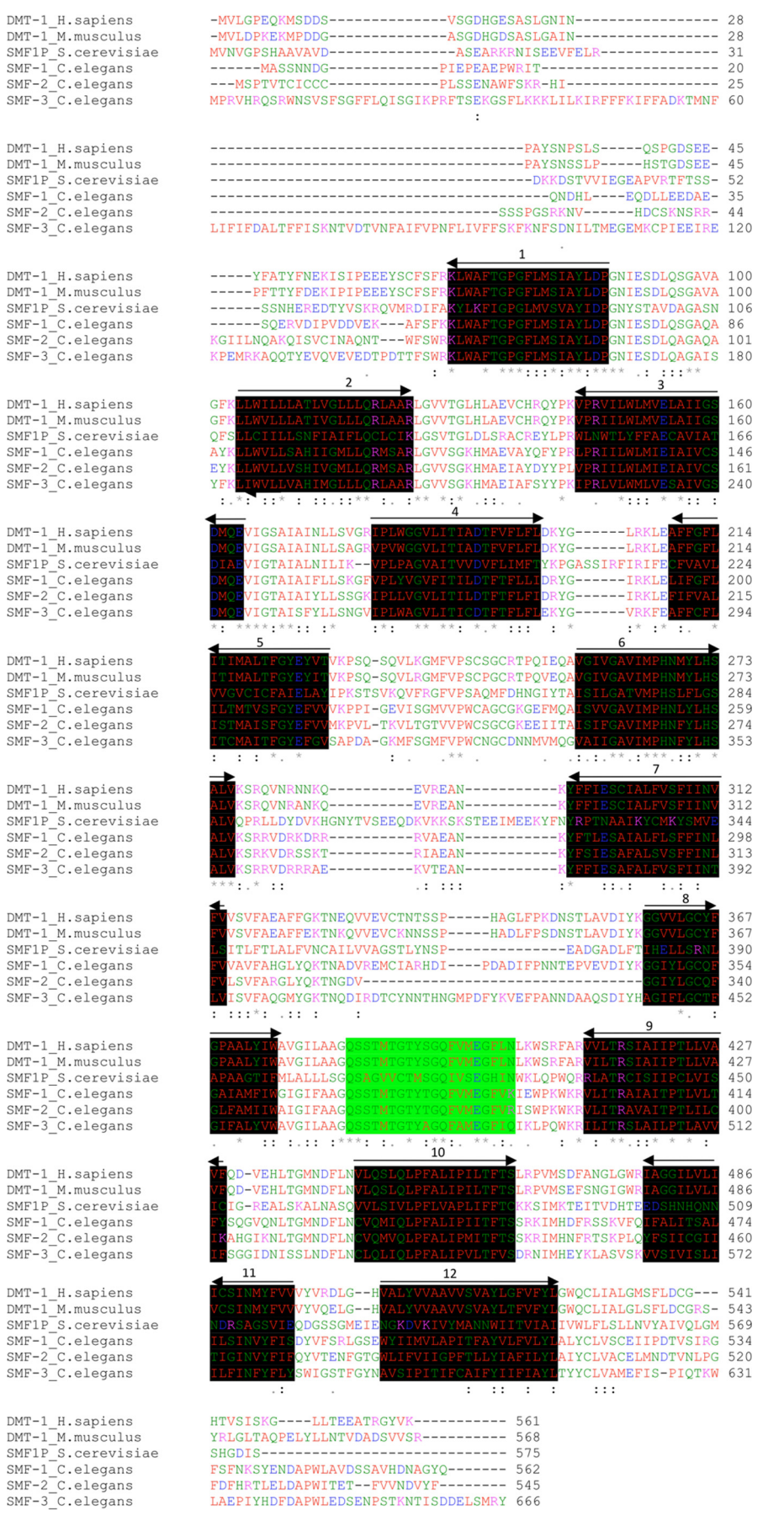

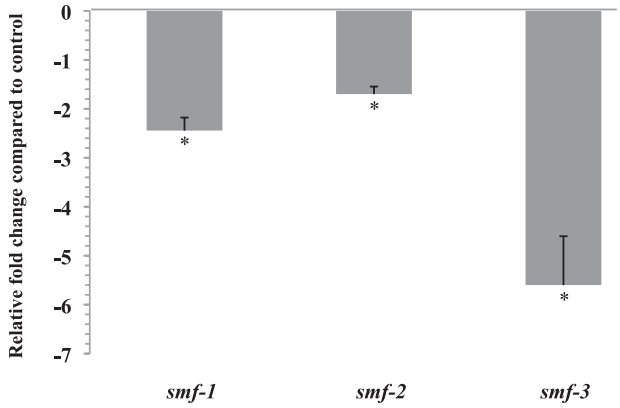

FIGURE 4. **Expression of *smf-1*, *smf-2*, and *smf-3* transcripts are modulated by exposure to Mn^{2+}.** L1 animals were exposed to 50 mM $MnCl_2$ for 30 min, mRNA-extracted, and reverse-transcribed to cDNA. Relative gene expression changes of *smf-1*, *smf-2*, and *smf-3* were quantitated using real-time PCR. The -fold change in gene expression relative to GAPDH was calculated for each gene following the $\Delta\Delta C_T$ method. Shown are mean values for -fold change ± S.E. of three individual replicates. *, indicates $p \leq 0.02$ between control and Mn^{2+}-treated group ΔC_T values.

rapid reduction of mRNA levels, ranging from ~1.8- to 5.0-fold change (Fig. 4) (supplemental Fig. S1). These results indicate that the gene expression is highly sensitive to environmental Mn^{2+} and suggest that the down-regulation of the putative transporters could be an attempt to limit cellular or cytoplasmic Mn^{2+} concentrations and toxicity.

SMF-1 and SMF-2 Are Expressed in DA Neurons—DMT-1 has recently been implicated in regulating Fe^{2+}-mediated DA neuron cell death *in vitro* and in PD (44). The transporter is also expressed in humans in DA neurons in the substantia nigra, and three homologues are expressed in yeast (73, 74). In yeast, Smf1p and Smf2p appear to be regulated by Mn^{2+}, while Smf3p may be regulated through a non-Mn^{2+} pathway (74). Each of the three putative homologues in *C. elegans* have primary and secondary sequence similarities characteristics with their yeast number counterparts, suggesting that the *C. elegans* SMF-1 or SMF-2 may be more likely to be involved in Mn^{2+} transport. To determine whether SMF-1 or SMF-2 is expressed in *C. elegans* DA neurons, we generated antibodies to both nematode proteins. To determine specificity of the antibodies and the role that the SMF proteins may play in Mn^{2+}-mediated DA neurodegeneration, we crossed our $P_{dat\text{-}1}$::GFP transgenic animals (BY250) into *C. elegans* strains that contain either a mutation in SMF-1 (IG6 *smf-1(eh5) X*) or SMF-2 (VC171 *smf-2(gk133) X*) resulting in strains RJ907 and RJ905, respectively. The *smf-1(eh5)* mutation contains a 2063-bp deletion in *smf-1* that results in a truncation of the protein beginning in transmembrane domain six. The mutation likely results in a null mutant, because the consensus transport sequence has been deleted. The *smf-2(gk133)* mutation contains a 448-bp deletion in the *smf-2* gene and likely results in a non-functional protein, because the deletion spans the start codon and the first three transmembrane domains. The morphology of the DA neurons in animals containing mutations in either *smf-1* or *smf-2* appear identical to those of BY250 (data not shown), suggesting that these transporters do not play a significant role in maintaining DA neuron integrity. To determine whether the DA neurons express SMF-1 or SMF-2, we generated primary cultures from BY250 animals. GFP is strongly expressed in DA neurons both *in vivo* and *in vitro* (49, 75). We used affinity-purified anti-SMF-1 to evaluate cellular SMF-1 expression levels. SMF-1 immunoreactivity is observed in DA neurons, as well as other cell types (Fig. 5, *A–D*). No specific staining was observed in DA primary neurons or other cells from *smf-1* mutant worms (Fig. 5, *E–H*). These results indicate that SMF-1 is expressed in DA neurons and that the antibody is likely specific for the putative transporter. As observed with SMF-1 immunofluorescence, SMF-2 is also expressed in DA neurons, as well as other cells, and the SMF-2 antibody did not immunoreact with other cells in the *smf-2* mutant primary cultures (Fig. 6, *A–H*). Taken together, these results indicate that SMF-1 and SMF-2 proteins are expressed in DA neurons and that animals containing the deletions within SMF-1 or SMF-2 likely do not express the proteins in their respective mutant backgrounds.

SMF-1 Contributes to Mn^{2+}-induced DA Neurodegeneration—Vertebrate DMTs transport divalent cations into the cell or intracellular compartments and may play a role in the generation of Mn^{2+}-induced oxidative stress (1, 76, 77). Because Mn^{2+} exposure can confer DA neurodegeneration, and SMF 1 and SMF 2 are expressed in DA neurons, we asked whether the putative transporters may contribute to Mn^{2+}-induced DA neuron vulnerability. Nematodes were grown for two generations on RNAi bacteria to reduce expression of either *smf-1* or *smf-2* or both genes together. Reduction in mRNA levels of *smf-1* or/and *smf-2* was confirmed by quantitative PCR (data not shown). RNAi of either *smf-1* or *smf-2* is also specific and robust, because knockdown of either protein resulted in loss of immunoreactivity with its corresponding antibody while not affecting the expression of the orthologue (supplemental Figs. S2 and S3). L1 larvae were exposed to 50 mM $MnCl_2$ for 30 min and allowed to recover on the RNAi bacteria for an additional 72 h, and DA neuronal morphology was evaluated. Animals in which *smf-1* gene expression was reduced show 42% more resistance to Mn^{2+}-induced DA neurodegeneration relative to WT animals (Fig. 7*A*). Furthermore, there was not a significant difference in Mn^{2+}-induced DA neuronal death between WT animals and animals with a reduction in *smf-2* expression. Ani-

FIGURE 3. **Sequence alignment of putative *C. elegans* DMT homologues with yeast and mammalian DMTs.** The sequences of human DMT (GenBank™ accession number NP_000608), murine Nramp2 (GenBank™ number L33415), yeast SMF1P (GenBank™ accession number NC_001147), *C. elegans* SMF-1 (GenBank™ accession number AAC46569), *C. elegans* SMF-2 (GenBank™ accession number AAC46568) and *C. elegans* SMF-3 (GenBank™ accession number AAL27264) were aligned using the ClustalW2 program following an NCBI BLAST search. The twelve putative transmembrane regions are highlighted in *black*; the *arrow* above the sequence indicates the orientation relative to the membrane, *i.e. right-directed arrowhead* = N-terminal to C-terminal, extracellular to intracellular. Consensus transport sequence located between transmembrane domains eight and nine are highlighted in *green*. The *red font* in the sequence represents hydrophobic amino acids, whereas *blue* represents acidic, *magenta* represents basic, *green* represents hydroxyl, and *gray* represents other types of amino acids. The *asterisk* indicates amino acids in that column are identical, *colons* represent conserved substitutions (same color group), and *periods* represent semi-conserved substitution (*similar shapes*). A BLAST search with the human homologue of DMT-1, and a sequence alignment of the results using ClustalW2 suggests that *C. elegans* has three putative homologues, SMF-1–3 (percent similarity from 69% to 76%, with percent amino acid identity between 53 and 58%).

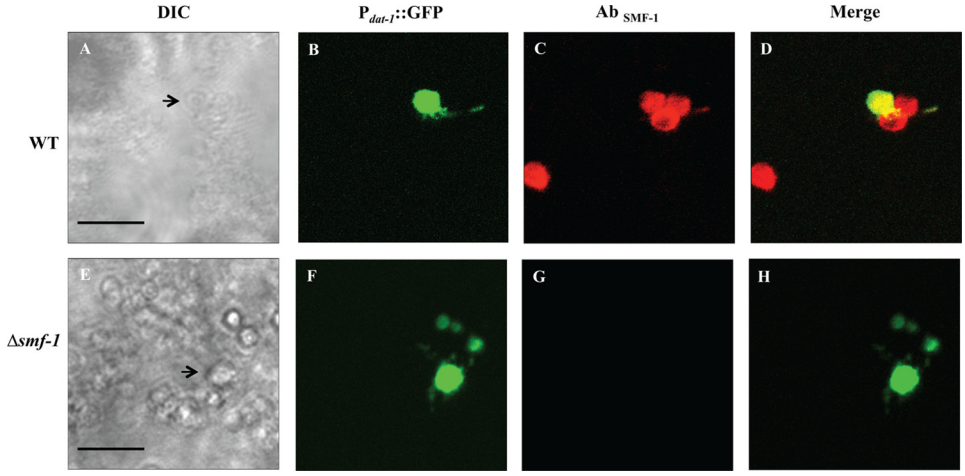

FIGURE 5. **SMF-1 is expressed in DA neurons.** Primary *C. elegans* cultures expressing GFP in the DA neurons were generated with WT (*A–D*) or *smf-1* mutants (*E–H*), and fixation was performed as described under "Experimental Procedures." Primary cultures were incubated with SMF-1 primary antibodies followed by incubation with Texas Red-conjugated goat anti-rabbit secondary antibodies. Differential interference contrast images of *A* and *E* of WT and *smf-1* mutant cultures, respectively, are shown. DA neurons from WT and *smf-1* mutants expressing GFP driven by the *dat-1* promoter *B* and *F*, respectively. SMF-1 colocalized with DA neurons in WT animals (*C*), but not in *smf-1* mutants (*G*). *D*, overlay of *B* and *C*; *H* overlay of *F* and *G*. Images were observed under a Zeiss confocal microscope (Zeiss LSM 510). *Scale bar* represents 45 μm.

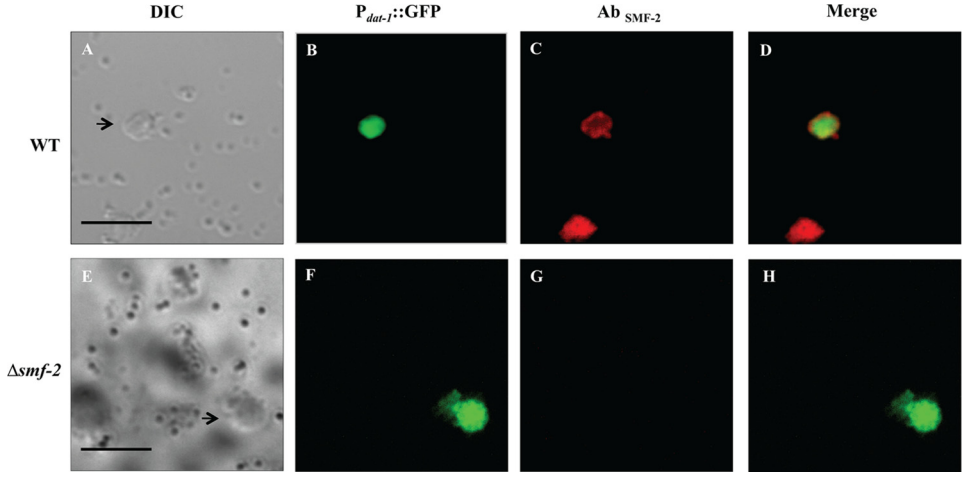

FIGURE 6. **SMF-2 is expressed in DA neurons.** Primary *C. elegans* cultures expressing GFP in the DA neurons were generated with WT (*A–D*) or *smf-2* mutants (*E–H*), and fixation was performed as described under "Experimental Procedures." Primary cultures were incubated with SMF-2 primary antibodies followed by incubation with Texas Red-conjugated goat anti-rabbit secondary antibodies. Differential interference contrast images of *A* and *E* of WT and *smf-2* mutant cultures, respectively, are shown. DA neurons from WT (*B*) and *smf-2* (*F*) mutants expressing GFP driven by the *dat-1* promoter. SMF-2 colocalizes with DA neurons in WT animals (*C*), but not in *smf-2* mutants (*G*). *D*, overlay of *B* and *C*; *H*, overlay of *F* and *G*. Images were observed under a Zeiss confocal microscope (Zeiss LSM 510). *Scale bar* represents 45 μm.

mals with a reduction in expression of both genes also did not decrease DA neuron vulnerability relative to the *smf*-1 knockdown, suggesting that *smf-2* does not compensate for the reduction in *smf-1* expression. To determine whether a probable functional deletion in either gene can protect DA neurons against Mn^{2+} toxicity, we exposed the mutant animals to Mn^{2+} and evaluated the DA neuronal integrity 72 h later. Consistent with our RNAi studies, the *smf-1* mutants were 40% more tolerant to Mn^{2+} relative to the WT animals (Fig. 7*B*). Furthermore, the likely functional deletion of SMF-2 did not decrease the vulnerability of DA neurons to Mn^{2+}. To determine whether SMF-3 may contribute to Mn^{2+}-induced DA neuronal death, we crossed the animals expressing GFP in the DA neurons with the likely *smf-3* functional deletion mutant RB1074; this transporter is likely non-functional, because the C terminus has a deletion that includes ~80% of the consensus transport sequence. DA neurons in animals containing the *smf-3* mutation were not more resistant to Mn^{2+} relative to WT (Fig. 7*B*). Taken together, these results indicate that expression of SMF-1 increased DA neuron vulnerability to Mn^{2+}, and neither SMF-2 nor SMF-3 contributed to the neurotoxicity.

SMF-1 and SMF-2 Contribute to 6-OHDA-induced DA Neurodegeneration—DMT-1 has recently been shown to contribute to DA neuron vulnerability in PD and vertebrate models, likely through an Fe^{2+}-dependent mechanism. To determine if SMF-1 or SMF-2 contributes to 6-OHDA-induced DA neuron degeneration in *C. elegans*, we knocked down gene expression of each of the genes as described above and exposed the animals for 30 min to 5 mM 6-OHDA as previously described (49, 58). Following a 72-h recovery, we found that animals that have reduced expression of *smf-1* or *smf-2* were 1.7 and 2.9 times more resistant to 6-OHDA-induced death than controls, respectively (Fig. 7*C*). Consistent with the RNAi studies, animals containing mutations within either SMF-1 or SMF-2 significantly protect DA neurons against the neurotoxicant (2.4- and 4.2-fold, respectively) (Fig. 7*D*). SMF-3 also does not appear to play a role in the toxicity, because deletion of the gene does not provide protection against 6-OHDA-induced cell death. These results indicate that both SMF-1 and SMF-2 play a role in 6-OHDA-induced DA neuronal death and provide further evidence that divalent cations contribute to PD-associated DA cell death.

DISCUSSION

Overexposure to Mn^{2+} can cause the neurological disorder Parkinsonism and has been implicated as an environmental toxicant that may contribute to the development of PD. Both disorders share a number of clinical and pathophysiological features that includes motor deficits, DA neuronal damage, and mitochondria dysfunction, which suggests that there may be overlapping modalities and molecular pathways that contribute to the pathologies. A difficulty in dissecting the molecular

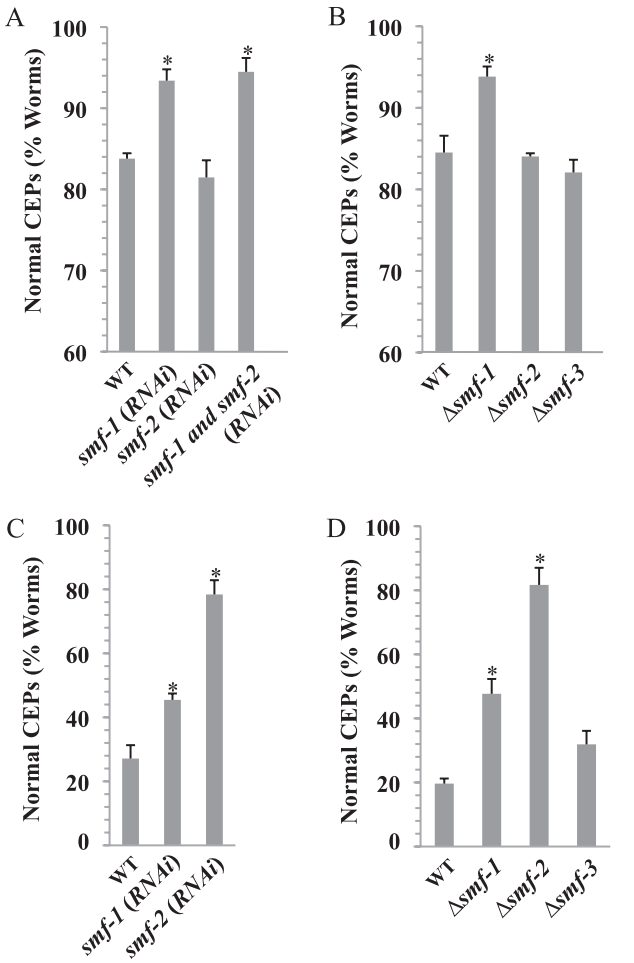

FIGURE 7. **SMF-1 contributes to Mn^{2+}-induced DA neurodegeneration, and SMF-1 and SMF-2 contribute to 6-OHDA-induced DA neuronal death in *C. elegans*.** Synchronized L1 WT and mutant *smf-1* and *smf-2* worms were exposed to either 50 mM $MnCl_2$ or 5 mM 6-OHDAfor 30 min and allowed to recover on NGM plates at 20 °C for 72 h as described under "Experimental Procedures." RNAi gene expression reduction (*A*) or deletion (*B*) of smf-1 confers partial protection against Mn^{2+}-induced DA neurodegeneration. RNAi gene expression reduction (*C*) or deletion (*D*) of both *smf-1* and *smf-2* conferred partial protection against 6-OHDA-induced DA neurodegeneration. SMF-3 does not contribute significantly to Mn^{2+}- or 6-OHDA-induced DA neuronal death (*B* and *C*). Shown are mean values ± S.E. of at least three individual replicates. *p* values were calculated using *t* test analysis. *, $p \leq 0.03$ between WT and mutants or RNAi worms.

determinants in both disorders includes the cellular complexity of the vertebrate brain and the lack of facile *in vivo* genetic models to dissect the molecular mechanisms involved in Mn^{2+}-induced DA neuron cell death. In this study, we describe a novel *in vivo* model for manganism and show that the *C. elegans* DA neurons degenerate following a brief exposure to Mn^{2+} (Fig. 2, *A–E*). We also show that SMF-1, a homologue of the vertebrate Mn^{2+} transporter DMT-1, is expressed in the DA neurons, and genetic knockdown or deletion of the transporter partially inhibits the neurodegeneration (Figs. 5 and 7). Considering the strong sequence similarities between SMF-1 and DMT-1, and the role SMF-1 plays in Mn^{2+}-induced cell death, our studies suggest that SMF-1 contributes to Mn^{2+}-induced DA neuron vulnerability by transporting the ion into the cell or into a Mn^{2+}-sensitive intracellular compartment.

DMT-1 has recently been found to be elevated in PD patients relative to age-matched controls and may contribute to the excess Fe^{2+} found in the mesencephalon associated with PD (44). DMT-1 has also been proposed to contribute to 1-methyl-4-phenyl-1,2,3,6-tetrahydropyridine- and 6-OHDA-induced DA neuron toxicity in rodents and primates by increasing cellular Fe^{2+} levels and by providing a catalyst for the Fenton reaction or Haber-Weiss reaction, whose products include the highly reactive hydroxyl radical that causes protein denaturation, lipid peroxidation, and cellular death (44, 78). Our studies also show that SMF-2 is expressed in DA neurons, and expression of either SMF-1 or SMF-2 dramatically increases DA neuron sensitivity to 6-OHDA (Figs. 6 and 7). These results suggest that the transporters may be facilitating neuronal death by the Fe^{2+}-catalyzed Fenton reaction. Mn^{2+} can also catalyze Fenton reactions, and SMF-1 could be contributing to the neurotoxicity as well through this molecular pathway (10, 79). Furthermore, Mn^{2+} exposure may increase expression of the transporters to allow greater Mn^{2+} influx, because Mn^{2+} has previously been shown to increase DMT-1 mRNA and protein expression in cultured choroidal epithelia (80). Although we find that an acute elevated exposure to Mn^{2+} decreases SMF mRNA levels immediately following the exposure (Fig. 4), examination of SMF-1 protein expression levels at later time points would provide insight into this mechanism.

SMF-1 or SMF-2 may also be involved directly or indirectly in the regulation of DA-associated proteins that could affect DA neuron vulnerability to the neurotoxicant. For example, Fe^{2+} regulation has been proposed to affect expression levels of DAT or tyrosine hydroxylase, the rate-limiting enzyme for dopamine (81). DAT transports 6-OHDA into DA neurons and has been proposed to play a role in DA neuron vulnerability to environmental toxicants (49, 82, 83). A reduction in DAT in the SMF mutant animals could result in lower quantities of toxicants entering the cell with a concomitant decrease in cell death. Tyrosine hydroxylase also requires Fe^{2+} as a cofactor, and a reduction in Fe^{2+} has been shown to decrease tyrosine hydroxylase and dopaminergic activity, which could result in decreases in susceptibility to DA neuronal insult (81, 84). Furthermore, DAT is also a target for Mn^{2+}, and exposure to Mn^{2+} has been shown to increase DAT surface expression that could result in increases in neuronal vulnerability (85).

α-Synuclein, a presynaptic protein of largely unknown function, was the first human gene identified in which a mutation appears to cause the development of (familial) PD (32, 33). Multiplications of the normal allele suggest that the gene is also a risk factor for the much more common sporadic (idiopathic) form of the disease. *In vitro* studies indicate that Mn^{2+} causes an increase in aggregation and fibrillation of α-synuclein, and greater cell death in cells expressing DAT (30, 70). Recently, suppression of α-synuclein-induced toxicity has been demonstrated by expression of the yeast or *C. elegans* orthologue of the human ATP13A2 (PARK9) (31). PARK9, a P-type ATPase associated with causing familial PD with dementia, localizes to lysosomes, and likely transports Mn^{2+} away from the cytoplasm into the intracellular compartment (86). Our studies show that DA neurons in nematodes exposed to Mn^{2+} and expressing WT human α-synuclein have an increase in DA neuronal death

relative to non-α-synuclein-expressing animals, consistent with vertebrate and cell culture studies (Fig. 2*F*). Furthermore, RNAi of *smf-1* in α-synuclein-expressing RNAi-sensitive nematodes alleviates the greater Mn^{2+}-induced DA neuronal death (data not shown), supporting the role of the transporter in the neurodegeneration. Abnormal Fe^{2+} and/or DA regulation as described above may also contribute to the α-synuclein-induced pathology (87, 88).

Acute Mn^{2+} exposure rapidly represses transcription of all three transporters, yet only SMF-1 appears to play a role in DA neuron sensitivity to Mn^{2+} (Figs. 4 and 7). The yeast Smf1p plays a significant role in cellular influx of Mn^{2+} largely when Mn^{2+} in the environment is limited (42). It is possible that SMF-1 protein expression levels in animals grown under normal laboratory conditions may also be higher relative to those grown in a Mn^{2+}-rich environment. Our studies involved exposing animals to high Mn^{2+} following incubation in an M9 synchronization buffer or following growth on RNAi media plates that contain <0.2 and 2.0 nM Mn^{2+}, respectively. Higher media Mn^{2+} concentrations may be more optimal for growth, considering an addition of up to 2 mM $MnSO_4$ can increase the rate of *C. elegans* development and brood size (89).

Excess exposure to Mn^{2+} in mammals *in vitro* and *in vivo* can confer oxidative stress and mitochondria dysfunction. Our studies also suggest that Mn^{2+} recapitulates vertebrate models. Pharmacological and toxicological studies in *C. elegans* are often performed at compound concentrations 10-fold or greater due to the difficulty of compounds crossing the moderately impermeable cuticle; intracellular concentrations of solutes, and K_i's and K_m's of proteins or compounds with their respective molecular targets though are often similar to those found in other eukaryotes (45, 47, 90). A single sublethal 50 mM Mn^{2+} exposure in the nematode also confers oxidative stress and mitochondria dysfunction as determined by increases in glutathione production and ROS and decreases in oxygen consumption and head mitochondria membrane potential (Fig. 1). Also, our initial studies indicate that *C. elegans* tissue harvested from agar plates contain ~48 nM Mn^{2+}.[3] Following a 30-min exposure to 50 mM Mn^{2+} and a 30-h recovery period (before DA neuron cell death is apparent), Mn^{2+} tissue concentrations are ~7 μM. Considering that non-Mn^{2+} challenged vertebrate tissue generally contains <4 μM Mn^{2+}, our studies suggest that *C. elegans* cellular and mitochondria Mn^{2+} sensitivities are similar to vertebrate systems (91).

In summary, our findings describe a novel genetic model for manganism. We show that Mn^{2+} causes oxidative stress, mitochondrial dysfunction, and DA neuron cell death in *C. elegans* and that the DMT-1 homologue SMF-1 significantly contributes to the cell death. We also show that SMF-1 and SMF-2 localize to the DA neurons and that knock down or deletion of either gene inhibits 6-OHDA-induced DA neurodegeneration. The development of this genetic model should facilitate the identification of molecules and pathways involved in PD-associated and Mn^{2+}-induced DA neuron dysfunction and death.

[3] R. Settivari, G. Filippelli, and R. Nass, unpublished observation.

Acknowledgments—We gratefully appreciate the technical assistance of Michelle Fullard, Marketa Marvanova, Shaoyu Zhou, and Randy Hunter. We are thankful to Eric A. Engleman and Gabriel Filippelli for assistance with determining C. elegans DA and Mn^{2+} concentrations, respectively. We also appreciate early discussions with Michael Aschner. Some of the strains were provided by the Caenorhabditis Genetics Center, which is supported by the National Institutes of Health Center for Research Resources.

REFERENCES

1. Burton, N. C., and Guilarte, T. R. (2009) *Environ. Health Perspect.* **117,** 325–332
2. Takeda, A. (2003) *Brain Res. Brain Res. Rev.* **41,** 79–87
3. Aschner, J. L., and Aschner, M. (2005) *Mol. Aspects Med.* **26,** 353–362
4. Hurley, L. S., Woolley, D. E., Rosenthal, F., and Timiras, P. S. (1963) *Am. J. Physiol.* **204,** 493–496
5. Abdel-Naby, S., and Hassanein, M. (1965) *J. Neurol. Neurosurg. Psychiatry* **28,** 282–288
6. Witholt, R., Gwiazda, R. H., and Smith, D. R. (2000) *Neurotoxicol. Teratol.* **22,** 851–861
7. Chia, S. E., Foo, S. C., Gan, S. L., Jeyaratnam, J., and Tian, C. S. (1993) *Scand. J. Work Environ. Health* **19,** 264–270
8. Rodier, J. (1955) *Br. J. Ind. Med.* **12,** 21–35
9. Jiang, Y. M., Mo, X. A., Du, F. Q., Fu, X., Zhu, X. Y., Gao, H. Y., Xie, J. L., Liao, F. L., Pira, E., and Zheng, W. (2006) *J. Occup. Environ. Med.* **48,** 644–649
10. Crossgrove, J., and Zheng, W. (2004) *NMR Biomed.* **17,** 544–553
11. Racette, B. A., McGee-Minnich, L., Moerlein, S. M., Mink, J. W., Videen, T. O., and Perlmutter, J. S. (2001) *Neurology* **56,** 8–13
12. Fishman, B. E., McGinley, P. A., and Gianutsos, G. (1987) *Toxicology* **45,** 193–201
13. Thiruchelvam, M., McCormack, A., Richfield, E. K., Baggs, R. B., Tank, A. W., Di Monte, D. A., and Cory-Slechta, D. A. (2003) *Eur. J. Neurosci.* **18,** 589–600
14. Domico, L. M., Zeevalk, G. D., Bernard, L. P., and Cooper, K. R. (2006) *Neurotoxicology* **27,** 816–825
15. de Bie, R. M., Gladstone, R. M., Strafella, A. P., Ko, J. H., and Lang, A. E. (2007) *Arch. Neurol.* **64,** 886–889
16. Holzgraefe, M., Poser, W., Kijewski, H., and Beuche, W. (1986) *J. Toxicol. Clin. Toxicol.* **24,** 235–244
17. Fahn, S. (2008) in *Parkinson's Disease: Molecular and Therapeutic Insights from Model Systems* (Nass, R., and Przedborski, S., eds) pp. 3–8, Elsevier Academic Press, New York
18. Gorell, J. M., Johnson, C. C., Rybicki, B. A., Peterson, E. L., Kortsha, G. X., Brown, G. G., and Richardson, R. J. (1999) *Neurotoxicology* **20,** 239–247
19. Zayed, J., Ducic, S., Campanella, G., Panisset, J. C., André, P., Masson, H., and Roy, M. (1990) *Can. J. Neurol. Sci.* **17,** 286–291
20. Barbeau, A. (1984) *Neurotoxicology* **5,** 13–35
21. Desole, M. S., Miele, M., Esposito, G., Migheli, R., Fresu, L., De Natale, G., and Miele, E. (1994) *Arch. Toxicol.* **68,** 566–570
22. Oestreicher, E., Sengstock, G. J., Riederer, P., Olanow, C. W., Dunn, A. J., and Arendash, G. W. (1994) *Brain Res.* **660,** 8–18
23. Dobson, A. W., Weber, S., Dorman, D. C., Lash, L. K., Erikson, K. M., and Aschner, M. (2003) *Biol. Trace Elem. Res.* **93,** 113–126
24. Parenti, M., Rusconi, L., Cappabianca, V., Parati, E. A., and Groppetti, A. (1988) *Brain Res.* **473,** 236–240
25. Erikson, K. M., Dorman, D. C., Lash, L. H., and Aschner, M. (2007) *Toxicol. Sci.* **97,** 459–466
26. Migheli, R., Godani, C., Sciola, L., Delogu, M. R., Serra, P. A., Zangani, D., De Natale, G., Miele, E., and Desole, M. S. (1999) *J. Neurochem.* **73,** 1155–1163
27. Zhao, F., Cai, T., Liu, M., Zheng, G., Luo, W., and Chen, J. (2009) *Toxicol. Sci.* **107,** 156–164
28. Higashi, Y., Asanuma, M., Miyazaki, I., Hattori, N., Mizuno, Y., and Ogawa, N. (2004) *J. Neurochem.* **89,** 1490–1497
29. Tomás-Camardiel, M., Herrera, A. J., Venero, J. L., Cruz Sánchez-Hidalgo,

M., Cano, J., and Machado, A. (2002) *Brain Res. Mol. Brain Res.* **103,** 116–129
30. Uversky, V. N., Li, J., and Fink, A. L. (2001) *J. Biol. Chem.* **276,** 44284–44296
31. Gitler, A. D., Chesi, A., Geddie, M. L., Strathearn, K. E., Hamamichi, S., Hill, K. J., Caldwell, K. A., Caldwell, G. A., Cooper, A. A., Rochet, J. C., and Lindquist, S. (2009) *Nat. Genet.* **41,** 308–315
32. Polymeropoulos, M. H., Lavedan, C., Leroy, E., Ide, S. E., Dehejia, A., Dutra, A., Pike, B., Root, H., Rubenstein, J., Boyer, R., Stenroos, E. S., Chandrasekharappa, S., Athanassiadou, A., Papapetropoulos, T., Johnson, W. G., Lazzarini, A. M., Duvoisin, R. C., Di Iorio, G., Golbe, L. I., and Nussbaum, R. L. (1997) *Science* **276,** 2045–2047
33. Cookson, M. R. (2009) *Mol. Neurodegener.* **4,** 9
34. Chen, J. Y., Tsao, G. C., Zhao, Q., and Zheng, W. (2001) *Toxicol. Appl. Pharmacol.* **175,** 160–168
35. Stredrick, D. L., Stokes, A. H., Worst, T. J., Freeman, W. M., Johnson, E. A., Lash, L. H., Aschner, M., and Vrana, K. E. (2004) *Neurotoxicology* **25,** 543–553
36. HaMai, D., and Bondy, S. C. (2004) *Ann. N.Y. Acad. Sci.* **1012,** 129–141
37. Garrick, M. D., Dolan, K. G., Horbinski, C., Ghio, A. J., Higgins, D., Porubcin, M., Moore, E. G., Hainsworth, L. N., Umbreit, J. N., Conrad, M. E., Feng, L., Lis, A., Roth, J. A., Singleton, S., and Garrick, L. M. (2003) *Biometals* **16,** 41–54
38. Papp-Wallace, K. M., and Maguire, M. E. (2006) *Annu. Rev. Microbiol.* **60,** 187–209
39. Supek, F., Supekova, L., Nelson, H., and Nelson, N. (1996) *Proc. Natl. Acad. Sci. U.S.A.* **93,** 5105–5110
40. Liu, X. F., and Culotta, V. C. (1999) *J. Biol. Chem.* **274,** 4863–4868
41. Luk, E. E., and Culotta, V. C. (2001) *J. Biol. Chem.* **276,** 47556–47562
42. Culotta, V. C., Yang, M., and Hall, M. D. (2005) *Eukaryot. Cell* **4,** 1159–1165
43. Hubert, N., and Hentze, M. W. (2002) *Proc. Natl. Acad. Sci. U.S.A.* **99,** 12345–12350
44. Salazar, J., Mena, N., Hunot, S., Prigent, A., Alvarez-Fischer, D., Arredondo, M., Duyckaerts, C., Sazdovitch, V., Zhao, L., Garrick, L. M., Nuñez, M. T., Garrick, M. D., Raisman-Vozari, R., and Hirsch, E. C. (2008) *Proc. Natl. Acad. Sci. U.S.A.* **105,** 18578–18583
45. Nass, R., Merchant, K. M., and Ryan, T. (2008) *Mol. Interv.* **8,** 284–293
46. Nass, R., and Settivari, R. S. (2008) in *Parkinson's Disease: Molecular and Therapeutic Insights from Model Systems* (Nass, R., and Przedborski, S., eds) pp. 347–360, Elsevier Academic Press, New York
47. Nass, R., and Blakely, R. D. (2003) *Annu. Rev. Pharmacol. Toxicol.* **43,** 521–544
48. Nass, R., Miller, D. M., and Blakely, R. D. (2001) *Parkinsonism Relat. Disord.* **7,** 185–191
49. Nass, R., Hall, D. H., Miller, D. M., 3rd, and Blakely, R. D. (2002) *Proc. Natl. Acad. Sci. U.S.A.* **99,** 3264–3269
50. Lakso, M., Vartiainen, S., Moilanen, A. M., Sirviö, J., Thomas, J. H., Nass, R., Blakely, R. D., and Wong, G. (2003) *J. Neurochem.* **86,** 165–172
51. Cooper, A. A., Gitler, A. D., Cashikar, A., Haynes, C. M., Hill, K. J., Bhullar, B., Liu, K., Xu, K., Strathearn, K. E., Liu, F., Cao, S., Caldwell, K. A., Caldwell, G. A., Marsischky, G., Kolodner, R. D., Labaer, J., Rochet, J. C., Bonini, N. M., and Lindquist, S. (2006) *Science* **313,** 324–328
52. Vartiainen, S., Pehkonen, P., Lakso, M., Nass, R., and Wong, G. (2006) *Neurobiol. Dis.* **22,** 477–486
53. Ved, R., Saha, S., Westlund, B., Perier, C., Burnam, L., Sluder, A., Hoener, M., Rodrigues, C. M., Alfonso, A., Steer, C., Liu, L., Przedborski, S., and Wolozin, B. (2005) *J. Biol. Chem.* **280,** 42655–42668
54. Springer, W., Hoppe, T., Schmidt, E., and Baumeister, R. (2005) *Hum. Mol. Genet.* **14,** 3407–3423
55. Brenner, S. (1974) *Genetics* **77,** 71–94
56. Hope, I. (ed) (1999) *C. elegans: A Practical Approach*, pp. 1–15, Oxford University Press, New York
57. Novillo, A., Won, S. J., Li, C., and Callard, I. P. (2005) *Integr. Comp. Biol.* **45,** 61–71
58. Nass, R., and Hamza, I. (2007) *Curr. Protoc. Toxicol.* 1.9.1–1.9.18
59. Kampkötter, A., Pielarski, T., Rohrig, R., Timpel, C., Chovolou, Y., Wätjen, W., and Kahl, R. (2007) *Pharmacol. Res.* **55,** 139–147
60. Schulz, T. J., Zarse, K., Voigt, A., Urban, N., Birringer, M., and Ristow, M. (2007) *Cell Metab.* **6,** 280–293
61. Yoneda, T., Benedetti, C., Urano, F., Clark, S. G., Harding, H. P., and Ron, D. (2004) *J. Cell Sci.* **117,** 4055–4066
62. Ehrenberg, B., Montana, V., Wei, M. D., Wuskell, J. P., and Loew, L. M. (1988) *Biophys. J.* **53,** 785–794
63. Zarse, K., Schulz, T. J., Birringer, M., and Ristow, M. (2007) *FASEB J.* **21,** 1271–1275
64. Bianchi, L., and Driscoll, M. (2006) *WormBook*, The *C. elegans* Research Community (on-line)
65. Simmer, F., Tijsterman, M., Parrish, S., Koushika, S. P., Nonet, M. L., Fire, A., Ahringer, J., and Plasterk, R. H. (2002) *Curr. Biol.* **12,** 1317–1319
66. Timmons, L., and Fire, A. (1998) *Nature* **395,** 854
67. Kamath, R. S., and Ahringer, J. (2003) *Methods* **30,** 313–321
68. Schulz, J. B., Lindenau, J., Seyfried, J., and Dichgans, J. (2000) *Eur. J. Biochem.* **267,** 4904–4911
69. Shi, M. M., Kugelman, A., Iwamoto, T., Tian, L., and Forman, H. J. (1994) *J. Biol. Chem.* **269,** 26512–26517
70. Pifl, C., Khorchide, M., Kattinger, A., Reither, H., Hardy, J., and Hornykiewicz, O. (2004) *Neurosci. Lett.* **354,** 34–37
71. Altschul, S. F. (1991) *J. Mol. Biol.* **219,** 555–565
72. Larkin, M. A., Blackshields, G., Brown, N. P., Chenna, R., McGettigan, P. A., McWilliam, H., Valentin, F., Wallace, I. M., Wilm, A., Lopez, R., Thompson, J. D., Gibson, T. J., and Higgins, D. G. (2007) *Bioinformatics* **23,** 2947–2948
73. Cellier, M., Privé, G., Belouchi, A., Kwan, T., Rodrigues, V., Chia, W., and Gros, P. (1995) *Proc. Natl. Acad. Sci. U.S.A.* **92,** 10089–10093
74. Portnoy, M. E., Liu, X. F., and Culotta, V. C. (2000) *Mol. Cell. Biol.* **20,** 7893–7902
75. Carvelli, L., McDonald, P. W., Blakely, R. D., and Defelice, L. J. (2004) *Proc. Natl. Acad. Sci. U.S.A.* **101,** 16046–16051
76. Bressler, J. P., Olivi, L., Cheong, J. H., Kim, Y., and Bannona, D. (2004) *Ann. N.Y. Acad. Sci.* **1012,** 142–152
77. Aisen, P., Enns, C., and Wessling-Resnick, M. (2001) *Int. J. Biochem. Cell Biol.* **33,** 940–959
78. Zhang, S., Wang, J., Song, N., Xie, J., and Jiang, H. (2009) *Neurobiol. Aging* **30,** 1466–1476
79. Watts, R. J., Sarasa, J., Loge, F. J., and Teel, A. L. (2005) *J. Environ. Eng.* **131,** 158–164
80. Wang, X., Li, G. J., and Zheng, W. (2006) *Brain Res.* **1097,** 1–10
81. Salvatore, M. F., Fisher, B., Surgener, S. P., Gerhardt, G. A., and Rouault, T. (2005) *Brain Res. Mol. Brain Res.* **139,** 341–347
82. Miller, G. W., Gainetdinov, R. R., Levey, A. I., and Caron, M. G. (1999) *Trends Pharmacol. Sci.* **20,** 424–429
83. Nass, R., Hahn, M. K., Jessen, T., McDonald, P. W., Carvelli, L., and Blakely, R. D. (2005) *J. Neurochem.* **94,** 774–785
84. Levenson, C. W., Cutler, R. G., Ladenheim, B., Cadet, J. L., Hare, J., and Mattson, M. P. (2004) *Exp. Neurol.* **190,** 506–514
85. Chen, M. K., Lee, J. S., McGlothan, J. L., Furukawa, E., Adams, R. J., Alexander, M., Wong, D. F., and Guilarte, T. R. (2006) *Neurotoxicology* **27,** 229–236
86. Ramirez, A., Heimbach, A., Gründemann, J., Stiller, B., Hampshire, D., Cid, L. P., Goebel, I., Mubaidin, A. F., Wriekat, A. L., Roeper, J., Al-Din, A., Hillmer, A. M., Karsak, M., Liss, B., Woods, C. G., Behrens, M. I., and Kubisch, C. (2006) *Nat. Genet.* **38,** 1184–1191
87. Brown, D. R. (2009) *Biochem. Biophys. Res. Commun.* **380,** 377–381
88. Olivares, D., Huang, X., Branden, L., Greig, N. H., and Rogers, J. T. (2009) *Int. J. Mol. Sci.* **10,** 1226–1260
89. Lin, Y. T., Hoang, H., Hsieh, S. I., Rangel, N., Foster, A. L., Sampayo, J. N., Lithgow, G. J., and Srinivasan, C. (2006) *Free Radic. Biol. Med.* **40,** 1185–1193
90. Rand, J. B., and Johnson, C. D. (1995) *Methods Cell Biol.* **48,** 187–204
91. Keen, C. L., Ensunsa, J. L., and Clegg, M. S. (2000) in *Metal Ions in Biological Systems* (Sigel, A., and Sigel, H., eds) pp. 89–121, CRC Press, Boca Raton, FL